THE PENNSYLVANIA STATE UNIVERSITY
SCHREYER HONORS COLLEGE

DEPARTMENT OF MECHANICAL ENGINEERING

DETERMINING THE THERMAL CONDUCTIVITY OF ADDITIVELY MANUFACTURED MATERIALS CONSTRUCTED USING STEREOLITHOGRAPHY

JACQUELINE TRAUTMAN
SPRING 2019

A thesis
submitted in partial fulfillment
of the requirements
for a baccalaureate degree in Mechanical Engineering
with honors in Mechanical Engineering

Reviewed and approved* by the following:

Karen Thole
Department Head of MNE and Distinguished Professor
Thesis Supervisor

Jacqueline O'Connor
Assistant Professor of Mechanical Engineering
Honors Adviser

* Signatures are on file in the Schreyer Honors College.

ABSTRACT

Additive manufacturing is the relatively new process of layering material to build objects. As it is still a relatively new technology, there is still a lot of research to be done to fully understand its properties and potential applications. Past research has shown that the material properties of additively printed parts, including plastics produced by using stereolithography (SLA), are affected by the method of manufacture and this thesis will examine whether that is also true for the parts' thermal properties. By modifying the variables inherent in additive manufacturing including layer size, print orientation, and cure time, this research will examine the effects on the thermal conductivity of the parts. The thermal conductivity of several additive samples with various combinations of independent variables was measured and shown to have significant differences. Evaluation determined that the most significant influence impacting the thermal conductivity is the cure time. A part that is not completely cured will have a lower conductivity than a part that has been fully cured. Due to the effects of this independent variable on the results, further studies will be needed to understand the full trends and effects of the other variables although postulates were developed. This research could be expanded by examining different additive manufacturing techniques and materials to determine if the trends discovered are universal or not.

TABLE OF CONTENTS

LIST OF FIGURES

LIST OF TABLES

ACKNOWLEDGEMENTS

I would like to begin by expressing my gratitude to Dr. Karen Thole and the entirety of the Steady Thermal Aero Research Turbine (START) Laboratory who supported this research. I am thankful for the opportunity you gave me and all the help along the way.

I also need to thank the now Dr. Jacob Snyder for all your input, support, and feedback along the way. I appreciate your patience and understanding as I took on this project and tried my hand at research for the first time.

Additional thanks should go to graduate student Antony Katona for not only letting me use your laboratory's equipment but also helping me make sense of my results along the way.

I also greatly appreciate the time and support I received from Dr. Jacqueline O'Connor, my Schreyer Honors Advisor. I am so grateful for the guidance and support over the past several years and would have struggled to complete this thesis without your writing tips and suggestions.

Chapter 1

Introduction

In recent years, researchers in academia and industry have discovered the values of additive manufacturing. Additive manufacturing is a relatively new method of creating new objects that differs from the traditional manufacturing methods including machining, molding, rolling, pressing, and more. Each of these techniques involve taking away from the material or applying force to deform the material into the desired shape, which is why these methods are now classified as subtractive manufacturing. Additive manufacturing is different, as an object is created by adding layers of material until a shape is formed, like a block of sticky notes. Unlike sticky notes, however, additive manufacturing is not limited to a block shape. Instead, the layers can form complex geometries that involve internal geometries that were otherwise not possible or at least very complicated with subtractive manufacturing techniques.

The reason for the interest in this method of manufacture is that additive manufacturing processes allow for much more creative structural designs. When creating new parts or even updating existing parts, engineers have more opportunities to design parts to fit specific functions, rather than having to worry about the manufacturing limits of the subtractive methods as well. They can also improve the designs to be both more space- and weight-efficient while working with additive manufacturing technologies and methods. The part shown in Figure 1 has been redesigned to optimize weight without sacrificing function. Up to 75% of the material used in a traditionally manufactured part can be eliminated by using additive manufacturing [1].

Figure 1: An example of a design with optimized weight [1]

While material properties are generally considered to be constant for a given alloy and operating conditions, previous research has determined that the manufacturing method used can affect the mechanical properties of various materials. Cold rolling, hot rolling, molding, and machining all affect the properties of materials and this trend has been proven to hold true for additively manufactured materials as well. Researchers have concluded that parts manufactured by the selective laser melting (SLM) process have poor fatigue performance, as demonstrated in Figure 2 [2].

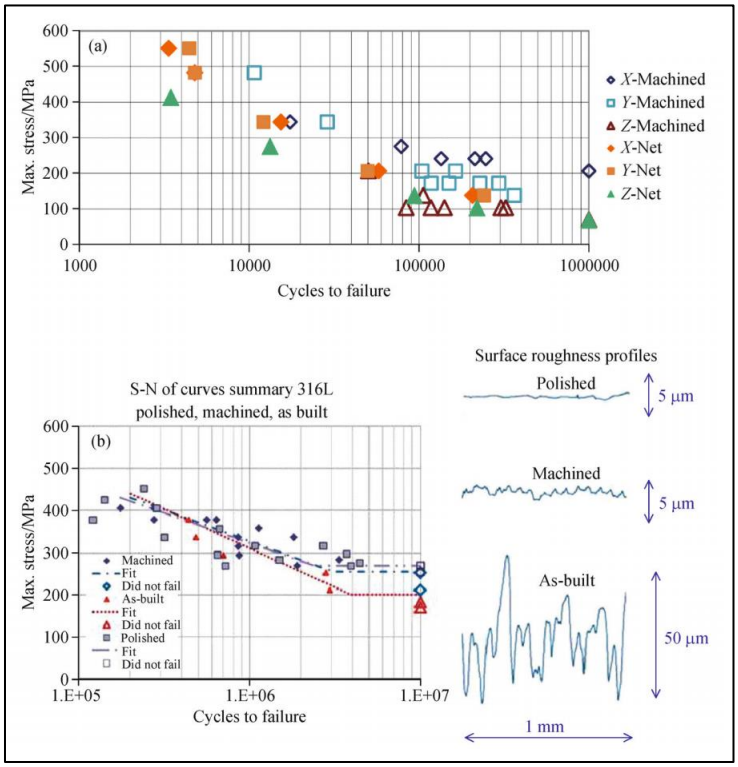

Figure 2: Differences in fatigue results of Selective Laser Melting processed (a) Ti-6Al-4V, and (b) 316L stainless steel due to method of manufacturing and test orientation [2]

Parts manufactured additively can sometimes perform better than those manufactured traditionally. Other research shows that Inconel 718 parts created using shaped metal deposition (SMD), laser, and electron beam (EB) processes outperformed the "as-cast" materials in yield strength and elongation as demonstrated in Table 1 [3].

Table 1: Ultimate Tensile Strengths, Yield Strengths and % Elongation of Inconel 718 [3]

AM Process	UTS, MPa	YS, MPa	% Elongation
SMD	828 ± 8	473 ± 6	28 ± 2
As-cast	786	488	11
Laser	904	552	16
EB	910	580	22

Studies on plastics, such as fused-deposition (FD) APS plastics have shown that the printing process naturally leads to some imperfections, namely small gaps or voids between the layers and a lack of a consistent molecular orientation. These lead to decreases in both the tensile

yield strengths and yield strains [4]. SLA is another method of printing plastic and similarly has specific trends in the properties of its printed parts. For SLA parts, there is high stiffness, but the parts tend to be very brittle and are prone to creep [5]. One of the benefits of SLA is that the parts are manufactured out of resin and companies manufacture different types of resin to promote different properties. Some resins build parts that have higher ductility, others have higher tensile strengths, and others are more resistant to large impacts. Examining the trends in these two types of printed plastics, the different printing processes influence the material properties of their prints.

These conclusions about mechanical properties raise the question: are the thermal properties also affected by the manufacturing processes and its many variables? While research has been done on the heat transfer concepts behind additive manufacturing [6] and the thermal processes involved in various additive processes and their effect on the quality of the construction [7], there are no readily available studies which demonstrate the effect of additive manufacturing on the thermal properties of the materials and parts being built.

To determine whether additively manufactured parts can safely and efficiently replace traditionally manufactured objects, no material properties can go unchecked. As there is an increasing demand for additively manufactured parts with heat transfer applications, it is critical that any differences in thermal properties are determined. The gas turbine blade with advanced cooling features shown in Figure 3 is just one specific example of a part where it would be important to know the thermal, as well as mechanical, properties of the building material—as turbine blades are expected to run in hot environments.

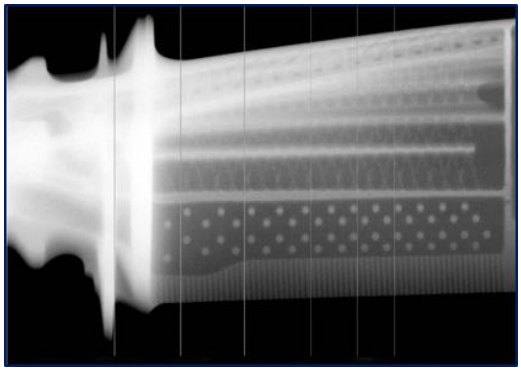

Figure 3: X-ray of a gas turbine blade showing internal cooling features [8]

The goal of this research is ultimately to determine if the thermal properties of an additively manufactured material are affected by variables such as layer thickness, print orientation, and cure time. This will be determined by measuring the thermal conductivities of a variety of printed parts. As part of answering that larger question, this thesis will focus on identifying the thermal conductivity for materials used in the Steady Thermal Aero Research Turbine (START) Laboratory, specifically, the "high temperature" plastic resin for the Form Labs Form2 SLA printer. Stereolithography abbreviated as (SLA) is an additive manufacturing methodology that utilizes a laser to cure a liquid resin to a solid state. The “high temperature” plastic resin being tested has literature verifying its mechanical properties but there is no value to refer to for thermal properties. Testing this plastic is important because critical test rigs and test articles are being produced with this material. Additionally, seeing the results of this experiment with simple test samples may help us analyze the results when in the future we move on to more complex test samples. Experimenting with variables such as layer thickness, cure time and print orientation will provide the lab with the information needed to understand how the test rigs will behave and provide some insight into any potential trends in thermal properties inherent in additively manufactured parts.

Chapter 2

Literature Review

Differences in Methods of Manufacturing

The additive manufacturing process is detailed extensively in the publication, "Additive Manufacturing Techniques in Manufacturing -An Overview", by Prakash et al. [9]. The research team introduces the key principles of additive manufacturing by outlining the way parts are built up "layer by layer" rather than using subtractive methods, which remove material to create the features of a part. Traditional manufacturing techniques place high emphasis on subtractive methods in order to create the defining features of a part. This means that most parts are formed from one continuous block of material or a few blocks adhered together. Additive techniques on the other hand are based on laying out many different layers, controlled by a computer aided design (CAD) program. This overview also gives a brief description of all the major manufacturing methodologies, a list of advantages the technology brings, and a quick glance at some industry applications for additive manufacturing.

A publication by X. Wang et al. [10] also illustrates the additive process with a greater focus on plastics and the methodologies most commonly used on plastics including SLA. This article centers around polymer composites and elaborates on the properties of additively manufactured parts. The article details the different materials used for each method of printing then goes further to discuss the effects of the addition of particles to the polymer matrix which can improve the accuracy of the printing process or affect the material properties depending on

the methods and materials used. Fundamentally this publication agrees with the work of Prakash et al. as the concept of layering is thoroughly examined and the effects of this method are deliberated. However, this paper elaborates on the methods of manufacture for plastic and composite polymers and begins to mention the relationship between additive manufacturing and the material properties of the constructed parts.

Differences in Other Material Properties

Additional studies have been conducted specifically on the mechanical properties of additively manufactured parts. One example is the paper "Mechanical properties of components fabricated with open-source 3-D printers under realistic environmental conditions" by Tymrak et al. [11]. This study focuses on ABS and PLA plastic parts' tensile strengths and elastic moduli. The variables the research team considered were extruder and platform temperature, print speed, nozzle diameter, and the cooling of the part. The authors of the paper comment that printing the same part in different directions can "significantly affect tensile strength" and support that claim with trails on both ABS and PLA parts constructed with different layer thicknesses and print orientations. Based on this conclusion, the team conducts the rest of their trials with the load applied parallel to the layers, the orientation which yielded the largest tensile strength.

A study that expanded upon the work of Tymrak et al. was conducted by Chockalingam et al. [12] in an article titled "Influence of layer thickness on mechanical properties in stereolithography." This study is particularly relevant as it focuses on SLA printing, which is also the topic of this thesis. The research team in this case sought to investigate what

relationships the layer thicknesses of 100, 125, and 150 μm had with the mechanical properties of the finished parts. Tests on the tensile, yield, residual, and impact strength were conducted upon SLA parts constructed of the specified layer thicknesses. This study ultimately concluded that the parts constructed of the smaller thickness layers had the greatest strength.

A separate analysis conducted by Wittbrodt, and Pearce [13] sought to investigate another variable that affects mechanical properties in "The effects of PLA color on material properties of 3-D printed components". This pair evaluated five different PLA colored plastics including white, black, gray, blue, and natural and found that the different colors achieve optimum crystallinity as well as tensile strength at various temperatures. The researchers attributed the differences to the varying chemical makeup of the dyes within each of the plastics which affected the material's properties as the plastic was heated, extruded, then cooled. This study adds on to the work of Tymrak et al. by contributing another variable that affects the material properties of 3D printed materials.

Thermal Properties

While the previous study by Wittbrodt and Pearce considered the effects of temperature on the mechanical properties of the finished parts, their research did not examine the thermal processes of additive manufacturing or the thermal properties of the parts. The paper "The Synthesis Of Thermally Stable Polymers: A Progress Report," written by J. Idris Jones [14] focuses on the creation of plastic polymers capable of withstanding temperatures upwards of 500°C. The goal of Jones' paper is similar to this one as replacing traditionally manufactured

parts with additively manufactured parts requires the new parts to survive and operate in the same environmental conditions as the previous parts. That being said, Jones' paper focuses on improving the durability of polymers and maintaining the parts mechanical properties and ultimately neglects the thermal properties of the finished parts.

The same cannot be said for the Flaata, Michna, and Letcher team [15], which raises questions about the thermal properties of additively manufactured parts. This paper mirrors the motives and justifications expressed above in this paper's introduction, however Flaata et al. placed their focus on ABS and PLA plastics used in Fusion Deposition Modeling (FDM), which is a methodology which utilizes extrusion. Extrusion-based additive manufacturing differs greatly in process from laser curing based methodologies, therefore the research conducted in the following paper on parts manufactured using SLA printing will be independent and unique from the research described in the paper written by Flaata and his team.

While these studies did not directly address the properties of SLA finished parts, they did highlight the fact that additively manufactured plastics need further examination. Only the study by Flaata et al. even addressed the thermal properties that should be considered when using additively manufactured parts. Based on the conclusions of these journal articles, SLA parts need to be examined in more detail to determine if the part's thermal properties, and thermal conductivity share a potential correlation with the part's method of manufacturing.

Chapter 3

Method of Measuring Thermal Conductivity

Thermal conductivity (k) is a material property and is specifies the degree to which the material will as allow heat to flow through it. Mathematically it is defined as the heat flow (Q) over a cross-sectional area (A) divided by the temperature difference(ΔT) over a known length or width(x).

$$k = \frac{Qx}{A\Delta T}$$

When trying to find the thermal conductivity experimentally, typically the known values are the area and length and the experimental process must include ways to accurately measure the heat flow and temperature gradient. There are several methods through which this can be achieved, and each is governed by the standards of the American Society of Testing and Materials (ASTM).

Available Methodologies

One method of measuring thermal conductivity is the guarded heat flow meter technique [16]. This method places the test specimen between a heat source and a cold sink with heat sensors on the faces of the specimen. The entire stack is compressed to ensure constant contact between each component of the system.

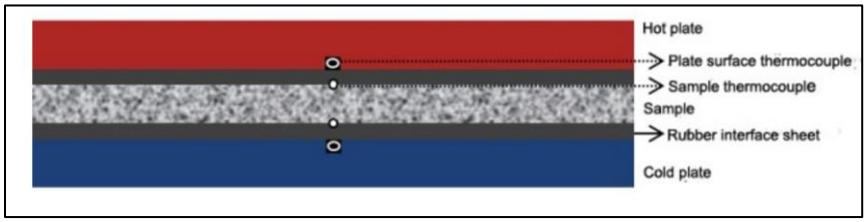

Figure 4: Specimen setup for a guarded hot-plate thermal conductivity test [17]

The voltage used by the heater is proportional to the heat flow through the specimen and the temperature sensors register the temperature gradient across the test piece, yielding both necessary unknowns to determine thermal conductivity. This system is commonly modified to adapt for different variables, such as type of testing material [18], the geometry of the test specimen [19], and the type of heat source [20]. While they have slightly different elements, each of these systems are classified under the guarded hot plate method, which is a steady state method because the equipment is taking data when the system is in an equilibrium state.

An alternative to the steady state method is the transient method. Systems utilizing this method vary the amount of heat applied to the test specimen and take data on how the system reacts. One example of a transient method to determine thermal conductivity is the transient-plane-source (TPS) method, which utilizes a heat sensor in the shape of a double spiral that also serves as the heat source to the system. This spiral sensor is then placed between two test specimens and data is collected over a specified time period [21]. Once again, the voltage expended can be used as the heat flow through the system. In this case, however, the calculations required are slightly different because the data collected shows the relationship of the temperature over time. Thermal conductivity can be calculated directly from the linear relationship between rise in temperature and the logarithm of time and thermal diffusivity, which can itself be calculated from density and other known factors [22].

Other transient systems exist where “High Speed Xenon-flash Delivery” sources or lasers are used to heat the samples. A pulse of energy is released and hits the face of the test sample, causing the temperature of the opposite face to rise as shown in Figure 5. This temperature increase is used in the calculations to determine the temperature gradient and heat flux across the sample [23].

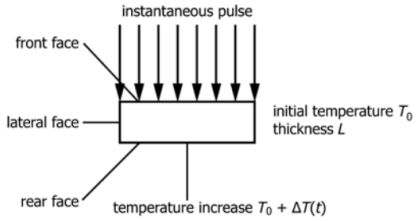

Figure 5: Diagram of the Flash method [23]

These systems can generate very accurate data on thermal conductivity as well as thermal diffusivity over very large temperature ranges. The flash systems are typically very sophisticated, however, and require the tests to be run in a vacuum. One disadvantage of this system is that establishing the vacuumed environment and generating large amounts of heat takes significant amounts of time [24].

After reviewing all these processes and their variations, the guarded heat flow method is a valid possibility for testing materials in the START lab. This method clearly reflects the heat transfer principles it is based upon and is adaptable, as seen by the many variations that have been developed. The limitations of the guarded heat flow method are the temperature range of about 150-600 K or -120 °C to 300 °C at which the system can operate, as well as the range of the thermal conductivity that it can detect. The systems typically reach their detection maximum at 30 W/m*K [25]. This is an allowable range for testing plastics, as almost all have thermal conductivities that fall within this range; but if the lab were interested in testing a wide variety of

metals, this limit would be problematic as certain metals can have thermal conductivities in the hundreds.

The transient plane source method could also be used, as its results are similarly accurate to those of the guarded heat flow method. It even has the advantage of yielding values for in-plane thermal conductivity in addition to through-plane conductivity. However, most systems require the researcher to know additional material properties to include density and heat capacity in order to determine the thermal conductivity [26].

If the lab's sole objective were to determine the thermal conductivity of all additively manufactured materials, the recommended method may be the xenon flash or a machine which utilizes a laser to heat the material samples. These systems can operate over an almost infinite temperature range and therefore can find thermal conductivities up into the thousands. These systems are incredibly expensive and go beyond wants and needs of the lab.

Evaluation

In order to determine the best methodology for the lab to use an in-depth comparison and evaluation of two potential machines was conducted. One machine was selected that embodied the guarded heat flow method and the other uses the transient plane source methodology. Below is a brief overview of the selected machine as well as an evaluation based upon their fit to the project's needs, accuracy, and cost.

DTC 300

The DTC 300 is a product of TA Instruments that can measure the thermal conductivity and other various thermal properties of a specimen. The instrument uses the guarded heat flow method in order to acquire its data. Figure 6 demonstrates how heat is applied to the test sample, which creates a temperature gradient through the specimen, and the variations in temperature over time are measured through a heat flow transducer and are used to calculate the thermal conductivity of the sample [27].

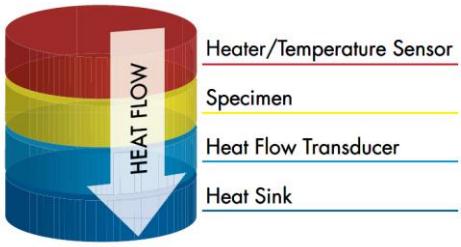

Figure 6: Demonstration of the theory behind the Guarded Heat Flow method [27]

In order to determine whether the DTC 300 fits the requirements of this research project, it must be determined that the instrument can handle samples of approximately one fourth of an inch thick and allow reasonable ranges for testing temperature and measuring thermal conductivity. According to the DTC 300 product sheet, the instrument can measure the thermal conductivity of specimen with a one-inch maximum thickness [27]. The research project favors smaller samples as printing large pieces can be quite expensive and time consuming and as no minimum size is provided the DTC 300 fits this requirement of the project. The TA instruments can operate at a temperature range of -20 °C to 300 °C, which also aligns with the project goals as this is a reasonable range with which we can determine if the additive manufacturing has any effect on the thermal conductivity. The measurable range of thermal conductivity is from 0.1 to 40 W/m*K [27].

The device's accuracy and precision will also play an important role in determining the superior testing instrument. TA Instruments guarantees an accuracy of ±3% to 8% and this claim is supported by the data provided by the sellers shown in Table 2 [27].

Table 2: Demonstration of accuracy given direct measurements to compare with literature values [28]

Thermal Conductivity (W/m·K)			
Temperature (˚C)	Direct Measurement	Literature Values	Error (%)
25	0.377	0.379	0.53
50	0.381	0.384	0.78
75	0.386	0.389	0.77
100	0.391	0.394	0.76
125	0.396	0.399	0.75
150	0.402	0.404	0.50
175	0.407	0.409	0.49
200	0.413	0.414	0.24
225	0.419	0.419	0.00
250	0.425	0.424	0.24
275	0.430	0.429	0.23
300	0.436	0.434	0.46

The percentage errors in Table 2 are considerably smaller than the guaranteed ±3% to 8%, which leads to the conclusion that the company has been intentionally conservative on its guarantees. The DTC 300 also claims a reproductability of ±1 to 2% indicating that any repeated trials should fall within 2% of themselves. The incredibly small percentage errors seen in the results verify the company's claim of accuracy as well as the guaranteed precision of the DTC 300. Therefore, the DTC 300 appears to be an appropriate instrument with which to conduct the research for this thesis.

While the START lab has not expressed an explicit budget for this research project, it can be assumed that minimizing expenditures when possible is always a benefit. With this in mind, the DTC 300 would cost the lab $83,000 to purchase and have delivered to the facility at CATO Labs [29]. In addition to this cost, the lab would be responsible for the costs of the materials and the manufacturing process for the testing samples to be used by the device. Exact numbers for

the samples cannot be given at this time until the exact sample sizes, materials, and additive method have been defined.

TPS 500

Hot Disk AB manufactures the TPS 500, which utilizes the Hot Disk Transient Plane Source (TPS) method in order to quickly gather thermal data on materials including the thermal conductivity [30]. This method is governed by ISO 22007-2:2015 and is recognized for being very precise or repeatable [28]. This method involves a very thin sensor made of a nickel wire wrapped in a Kapton coating which is placed between two sample parts [33]. When current moves through the wire coil as seen in Figure 7, the sensor encounters resistance from both the wire and the materials around the sensor.

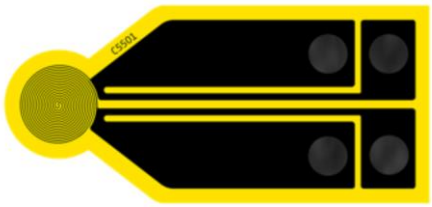

Figure 7: A sample "Hot Disk Sensor" used by the TPS 500 [30]

This resistance is measured and used to calculate the thermal conductivity of the material. The sensor is categorized as a hot disk sensor as the resistance created within the wire creates a small output of heat.

While the TPS 500 has no size limits listed on its product information page, we can determine that the samples used for this instrument must be at around 6 mm thick by examining

the various sensor sizes [30]. This instrument requires slightly thicker samples and twice as many samples as the DTC 300 due to the need to sandwich the sensor. While the increased sample size and number make this system not as cost and time efficient as the previous instrument, the parameters are not unreasonable and still fit the needs of the project. The usable temperature range for this device is -100 °C to 200 °C, which does not go quite as high as the previous system. Once again though, the tests to be run during this project should not need to be run under extremely high temperatures to determine whether there is a varying trend in the material's thermal conductivity. The TPS 500 does have an advantage in its range of measurable thermal conductivities. The TPS 500 range goes from 0.04 to 100 W/m*K which demonstrates a better resolution as well as a larger range [30]. While the DTC300 can get by with its thermal conductivity range, the TPS 500's range allows for more experimentation with different types of materials.

The TPS 500 is guaranteed to have an accuracy of "better than 5 %" according to the instrument's product page [30]. As seen by the guaranteed accuracy above, companies tend to be conservative in its percent error guarantees therefore this claim is particularly impressive. The TPS 500 also boasts a reproductability of 2% for its measurements of thermal conductivity. Both statements are incredibly like those of the DTC 300 therefore the TPS 500 also seems to be accurate enough for the measurements required for this research. If there is a trend that is not detected by either of these measurement devices.

While the TPS 500 would typically cost the START lab $76,000 including cost of purchase and delivery these costs can be effectively eliminated because a Penn State lab already owns one [29]. Graduate student Anthony Katona acquired a TPS 500 for his research but is no longer using the instrument regularly and volunteered unlimited access to the system for no cost.

While this machine's sandwiching method will double the cost for manufacturing samples, this added cost is insignificant compared to the alternative cost of buying the DTC 300. The larger range of thermal conductivity also allows for the potential for additional materials to be tested beyond the scope of the DTC 300, which could also increase the costs for both manufacturing and materials. This added expense is incomparable to the money the lab could save by working with the TPS 500.

Conclusion

After a thorough evaluation of both instruments, both appear to be strong candidates as potential solutions. The TPS 500 is the better solution given the established criteria. While this Hot Disk AB product does impose a few more limitations on the size of the samples to be used and the temperature range for this research, it has the greater measurable thermal conductivity range. This is significant as it increases the number of potential materials which can be tested an included in this study. Both the TPS 500 and DTC 300 appear to possess an accuracy that would meet the requirements of the project, although the TPS 500 claims a higher degree of accuracy according to the manufacturers. Finally, the TPS 500 has proven to be incredibly convenient as there is already one on campus eliminating the lab's need to purchase the instrument all together. While this instrument may require more samples of larger volumes, the TPS 500 is still the better financial choice by far. After considering each of these criteria, the TPS 500 is the instrument that should be used to study the potential correlation between additive manufacturing and a part's thermal properties.

Chapter 4

Research Results and Analysis

After determining that the TPS 500 would be the most realistic choice to use in the determining of the thermal conductivity of additively manufactured parts, the research could begin. The first step was to ensure that the TPS 500 was indeed the right machine for the project therefore a benchmark test was conducted to validate the machine and testing process.

Procedure

1. Load computer software for TPS 500 and select new batch to create an experiment
2. Click on the left most image labeled “Bulk (Type I) making sure that there are no checkboxes checked and the “Isotropic” option is selected in the popup window
3. Use the tips and tricks listed in Appendix A to properly adjust the settings of the test.
4. Ensure sensor is properly centered on four dots on the adaptor cord and clamp the sensor with the given materials, as in Figure 8.

Figure 8: Proper configuration of sensor assembly (steps – left to right)

5. Load sample pieces to be measured onto the test apparatus keeping the sensor horizontal, by raising the platform if necessary, and centering it between the two sample pieces like a sandwich

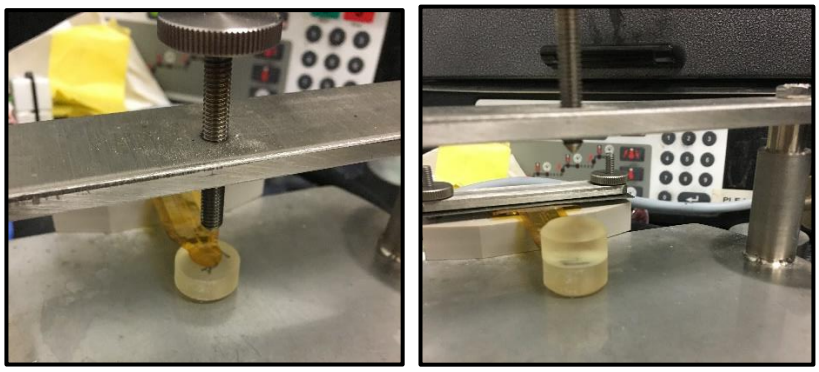

Figure 9: Proper positioning of samples on test rig

6. Tighten the screw at the top of the test rig in order to ensure full contact between the sensor and test pieces, as in Figure 9.
7. Start the experiment and click “OK” to the pop-up confirmation box that appears checking for an appropriate resistance reading as outlined in Appendix A
8. When the test is complete, click Calculate to gain access to the “Drift” and “Transient” windows as well as the results of the experiment, which will appear in the bottom right hand corner
9. Check for any inconsistencies or possible errors listed in Appendix A
10. Wait at least 36 times the length of the measurement time between runs to allow the material and sensor to return to steady state conditions
11. Rerun the experiment by right clicking the run in the bottom left window and creating a copy which will create a new run with the same settings
12. Collect at least five data points for proper analysis

Benchmark Test with Pyrex Sample

In order to test the accuracy of the TPS 500 two pieces of 10 mm thick Pyrex were bought to compare the TPS results with the known value. Pyrex was selected as an appropriate benchmark as its thermal conductivity is lower than other benchmarking materials, stainless steel for instance. This lower thermal conductivity is closer in range to the expected values of the SLA plastic. All thermal conductivities of materials depend on temperature and the thermal conductivity of Pyrex has been thoroughly mapped by several researchers. Therefore, there is a small range for the thermal conductivity at 25 °C but an accurate mid-range value for the thermal conductivity of Pyrex glass is 1.143 W/(m*K) at 25 °C [31]. The thermal conductivity values measured by the TPS 500 using the 3 mm sensor, which was used on the later samples, averaged to 1.18798 W/(m*K) with a confidence interval of 0.000557, which is equivalent to a 0.046858% confidence level from five data points. This means that based on the data the thermal conductivity was equivalent to 1.18798±0.000557 W/(m*K) and the % confidence indicates the relation between the size of the confidence level compared to the value of the measured value itself therefore a lower % indicates a higher level of confidence in the results.

The percent difference between the expected value and the measured value is approximately 3.8%. While not perfect, the measured value was comparable to the expected value and with the calculated confidence level any effect the independent variables have should be visible in the numbers. Therefore, the next step was to begin trials with additive parts.

Repeatability

Before continuing to the rest of the experiment, it is imperative to establish the repeatability of the measurements obtained with the TPS 500 on the SLA printed samples. The figure below demonstrates two measurements conducted on the same sample a month a part on the same machine.

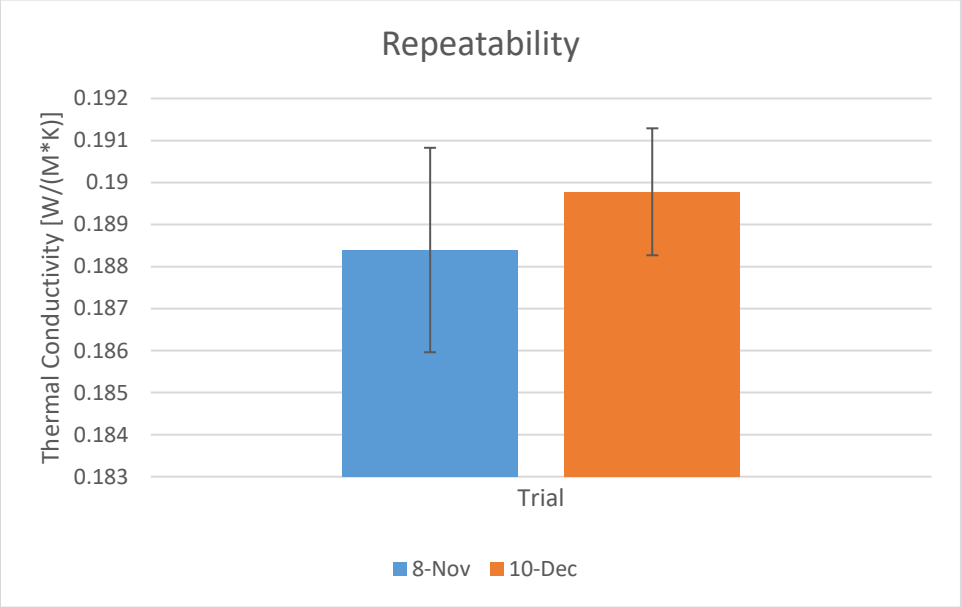

Figure 10: Repeatability analysis conducted on Sample F

The values are not identical however the confidence intervals calculated over five data points indicated by the error bars make it clear that it can be confidently stated that the measurements obtained following the above procedure will yield repeatable results. Note that the y-axis here has been adjusted so that the overlap in the error bars is clearly visible. The confidence levels in both cases are ±0.0006 and ±0.003, which are both equivalent to less than 2% of the thermal conductivity values measured.

Round 1: The Initial Study

The START Lab uses the Form II printer to create their test rigs out of Form Lab's High Temperature resin [32]. As the lab needs to know the thermal conductivity of the rig before they can begin testing the actual test samples, this high temperature resin will be the material used in the experiment. When working with the Form II printer, there are specific variables that are possible to control. This specific printer allows control of the layer thickness of the parts, so this experiment will focus on two different standard sizes that the lab uses in order to determine whether this variable influences the thermal conductivity.

One of the advantages of 3D printing is the ability to arrange your designs on the build tray in any orientation you see fit. Usually you arrange your parts to minimize print time, maximize stability, decrease the amount of material used to support the final design in the final print orientation, or to simply fit your design into the printer. Allowing that there can be variation in the build orientation means that it is important to determine whether the final build angle of the collective layers influences the manner in which heat transfers through a part. With this in mind, the experiment will include horizontal, vertical, and 45° oriented variations for both layer thicknesses tested.

Another step in the SLA printing process is curing. After the resin has been set by the UV laser and the printer finishes its work the parts get moved to a machine that will completely cure the parts by exposing them to more UV light. In order to determine if this additional curing process influences the thermal properties of the part the experiment requires one sample to remain uncured to act as a control. The final variable that the experiment will account for is the location of the build tray that the part is built on. As the tray of resin is used for multiple prints

the laser can leave a shadow on the glass build tray. Therefore, the experiment will include identical samples placed at different locations on the build tray to determine if the coordinates of the print have any effect on the properties of the part. All these variables and the various combinates are outlined in the test matrix outlined below.

Table 3: Round 1 Test Matrix

Sample	Layer Thickness	Print Orientation	Cure Time
A	100µm	horizontal	Standard cure
B	100µm	horizontal	Standard cure
C	100µm	horizontal	Standard cure
D	100µm	horizontal	Standard cure
E	100µm	horizontal	No post cure
F	100µm	vertical	Standard cure
G	100µm	45 degrees	Standard cure
H	25µm	horizontal	Standard cure
I	25µm	vertical	Standard cure
J	25µm	45 degrees	Standard cure

The results of these samples are as follows.

Table 4: Average thermal conductivity value and confidence level for five measurements per sample

Sample	Thermal Conductivity [W/(m*K)]	Confidence (± [W/(m*K)])
A	0.16899	0.00092
B	0.187368	0.001088
C	0.194137	0.003371
D	0.17256	0.000226
E	0.17874	0.000475
F	0.189779	0.001511
G	0.219142	0.003292
H	0.190548	0.000602
I	0.18849	0.000154
J	0.189894	0.000471

The first analysis to conduct is upon the effects of the layer thickness and print orientation variables as seen in Figure 11,which includes data from samples A, F, G, H, I, and J.

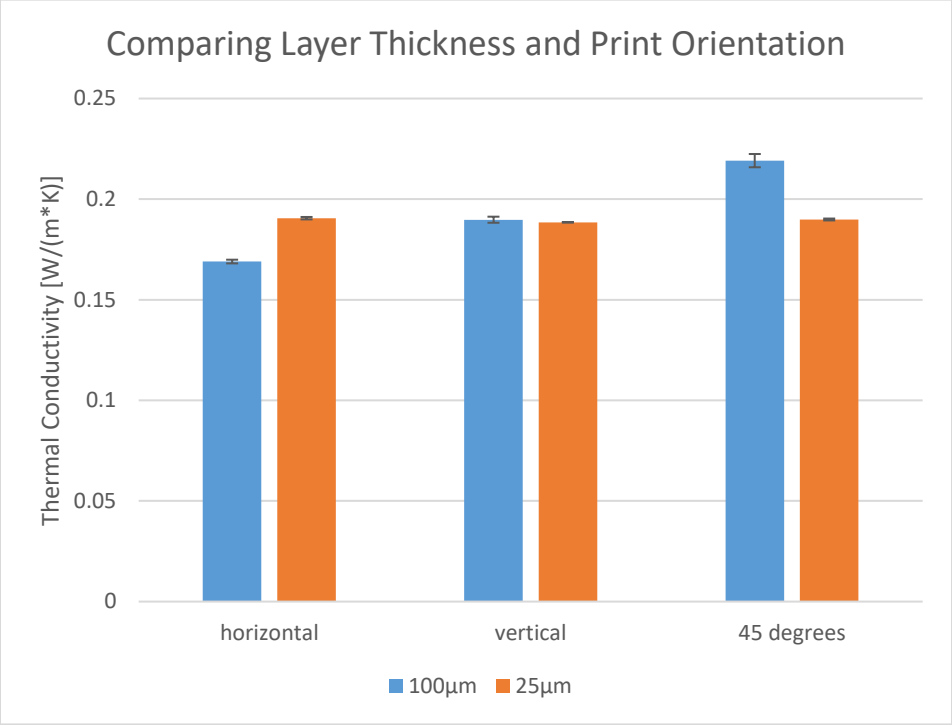

Figure 11: Comparison of Results from varying Layer Thickness and Print Orientation

These results also demonstrate high levels of confidence. However, in this case, the error bars do not all overlap, therefore it can be stated that there is a significant difference between the values. Sample A has the lowest value on this graph at 0.169 W/(m*K) while the highest sample, G, is 0.219 W/(m*K). The percent difference between these two values is 25.77%, which is significantly higher than the established repeatability limit; therefore, we can conclude that there is a difference in these results beyond the error of the measurements.

The measurements from the 25 µm samples are relatively consistent, while the variation demonstrated in the 100 µm samples are more extreme. This difference could mean that the smaller layers allow for a more uniform connection between the resin molecules regardless of the

print orientation, while the larger 100 μm layers do not have the same linking between the layers. It is possible that these more distinct layers affect the manner in which heat flows through the plastic, allowing better conduction along the layers rather than from one layer to another. This would explain the larger thermal conductivity in the vertically printed samples as the heat can travel more easily up the short layers. The 45° sample yields even higher results than the vertical, as the layers can conduct heat along the layers and the sample has a larger surface area to allow conduction between the layers as well, combining the heat transfer methods of the horizontal and vertical prints.

Figure 12 illustrates the results of samples A through E as the effects of location and cure time are evaluated. All the samples included have a layer thickness of 100 μm and were printed horizontally and only vary by print location. Sample E, which is visible on the far right, is different in that it has not received the standard post cure procedure.

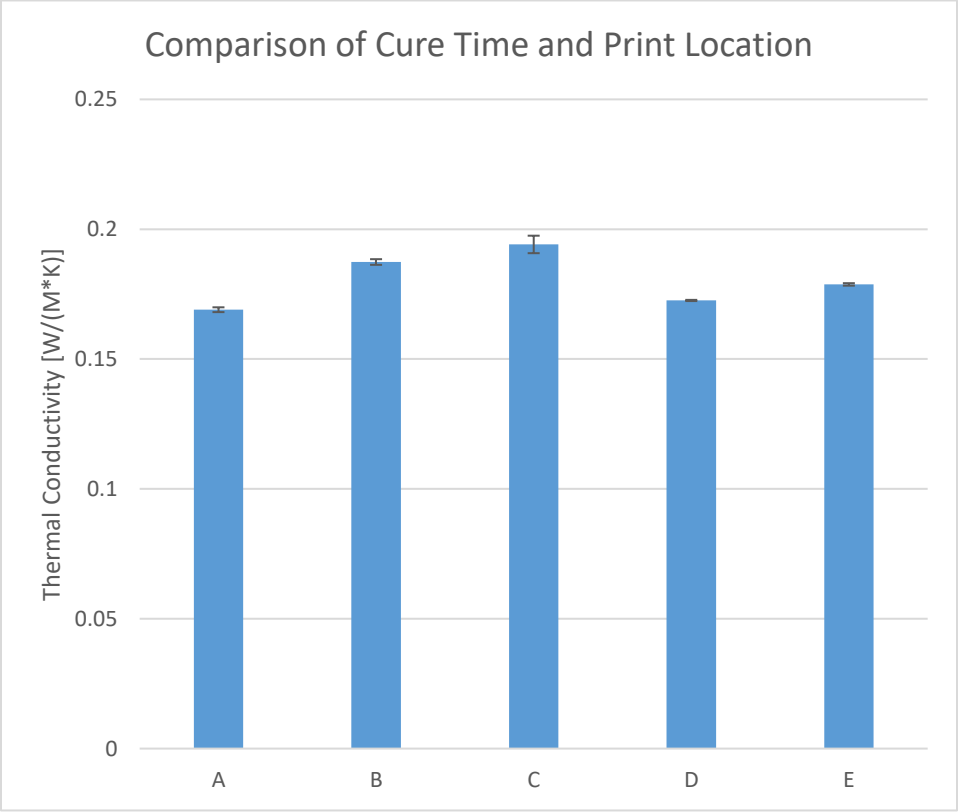

Figure 12: Comparison of samples with varied Print Location and Cure Time

The variation visible among these samples is extreme and required more investigation. In order to justify the difference between these values the print tray used to produce these samples was examined for shadows or other variations, as shown in Figure 13.

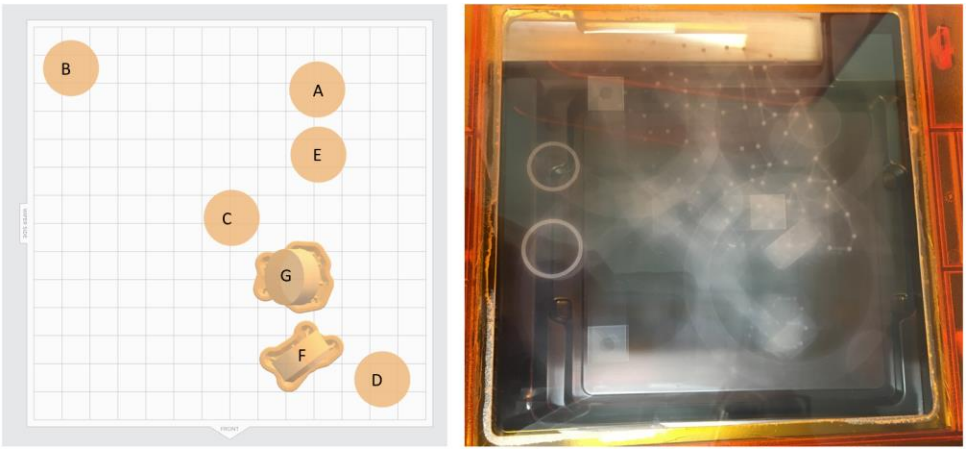

Figure 13: Examination of Print Locations (Left) and Build Tray (Right)

The aforementioned shadows are quite visible on the build tray as seen on the right of Figure 13. When comparing the samples to their shadows, no obvious pattern emerges. The shadows for samples C, E, and D are all quite prominent in comparison to A and B; however, the conductivity values are still quite different, and no pattern is revealed. These results were a cause for concern as no justification for the variation in measurements was readily available. Additionally, if the location and cure time yielded these extremely different values, the ability to judge the other variables independently came into question.

Round 2: The Targeted Study on the Effect of Print Location and Cure Time

In order to better understand the variation in the measurements, new 100 µm sample pieces were printed on a new and clean build tray in the same locations and the new samples were measured using the TPS 500. These samples are defined in the test matrix table.

Table 5: Test Matrix - Round 2

Sample	Layer Thickness	Print Orientation	Cure Time
2A	100µm	horizontal	Standard cure
2B	100µm	horizontal	Standard cure
2C	100µm	horizontal	Standard cure
2D	100µm	horizontal	Standard cure
2E	100µm	horizontal	No post cure
2F	100µm	vertical	Standard cure
2G	100µm	45 degrees	Standard cure

Results from these samples can be found in the table below.

Table 6: Average thermal conductivity value and confidence level for five measurements per round 2 sample

Sample	Thermal Conductivity [W/(m*K)]	Confidence (± [W/(m*K)])
2A	0.199632	0.0002823
2B	0.186596	0.0012042
2C	0.18715	0.0015979

2D	0.172597	0.0126552
2E	0.17879	0.0027328
2F	0.188226	0.0027474
2G	0.209269	3.255E-05

The visualization of the results for samples 2A through 2E are shown below.

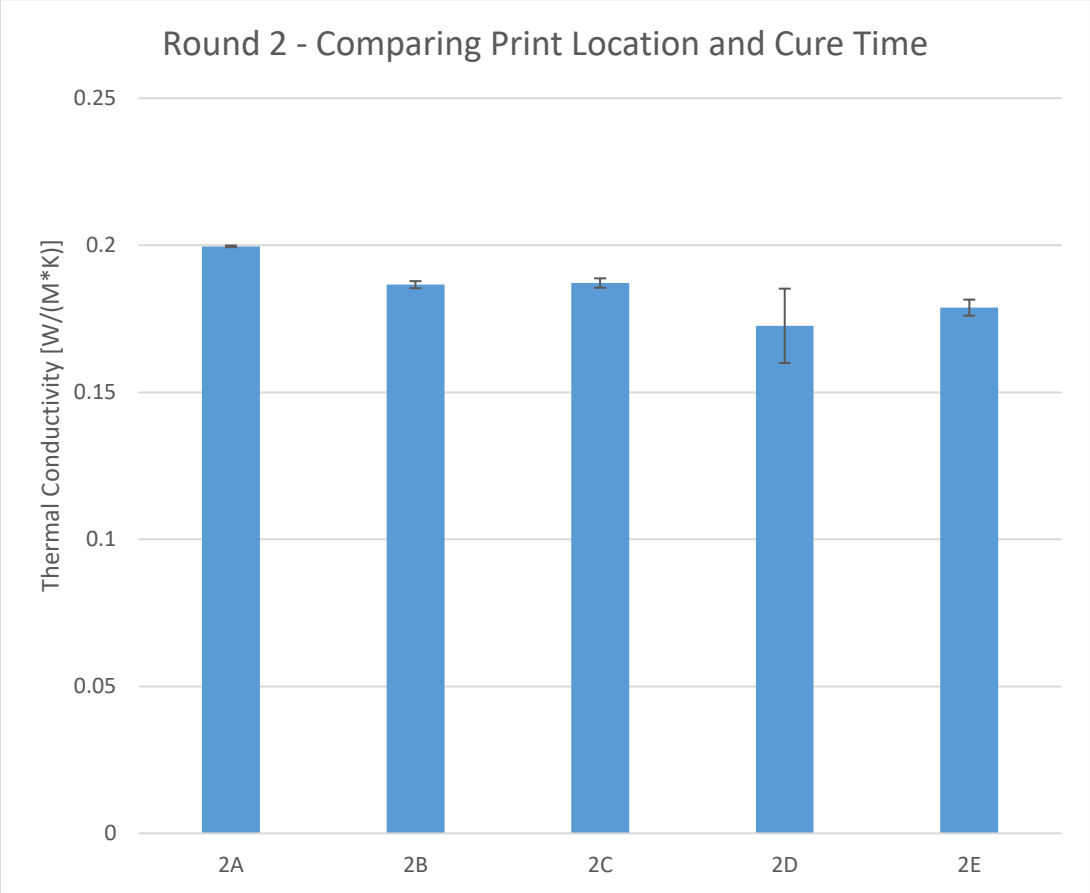

Figure 14: Round 2- Comparing Print Location and Cure Time

These measurements also demonstrate some variation, although less than the first round. Since these samples were created from a new tray, the hypothesis that the variation was due to the build tray shadows could officially be eliminated. At this point the concern arose that the issue was with the procedure rather than an observable trend. In an effort to find some

continuing trend among any of the data, all the 100 µm samples from rounds 1 and 2 were compared.

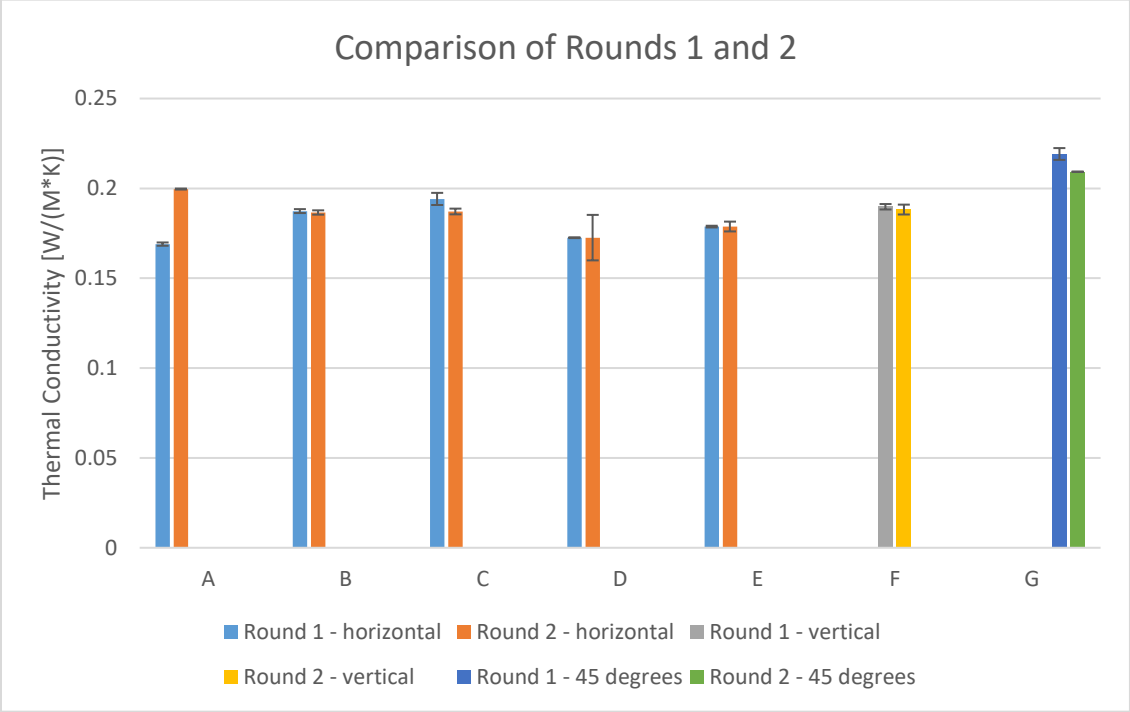

Figure 15: Rounds 1 and 2 - 100µm sample pieces

This comparison clearly illustrates a connection between location on the build tray and the thermal conductivity of the pieces. While samples A, C, and G have some discrepancies, the samples from both rounds still show remarkably similar results.

It was at this point that the cure time variable came under closer examination. Sample E showed distinct results in both rounds 1 and 2. As the relevance of the cure time came into question a closer evaluation of the curing process was conducted. One of the effects of the curing process was identified as a visible color change of the sample parts. The specimen that have been exposed to less light are of a lighter pigment than those which have been exposed to the curing process. Figure 16 shows samples 2E (2.2), A (1), and 2A (2.1) to illustrate the color gradient involved.

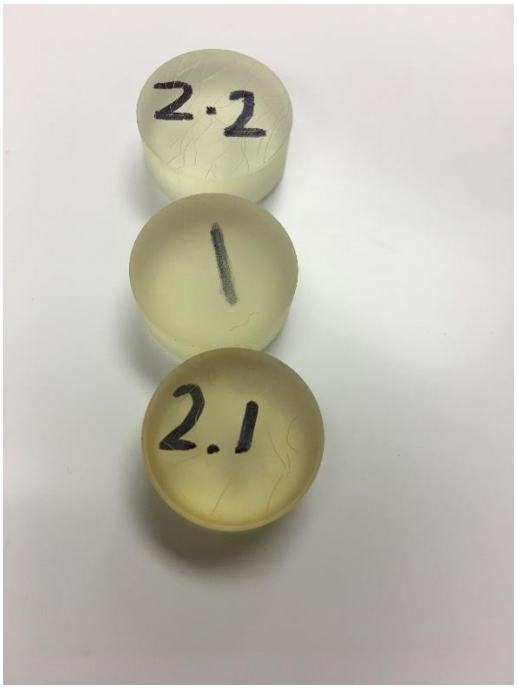

Figure 16: Curing Color Gradient

Sample 2A is about the same color as the rest of the samples and sample 2E is completely uncured, making it the lightest.

Sample A appears to have a pigment that does not match either sample 2A or 2E. It has experienced some curing, as indicated by the beginning of the color change; however, it has also not reached the full color change of the fully cured samples. The conclusion based on this deduction is that for some reason sample A seems to have experienced the curing process differently from the other fully cured samples. This observation corresponds to the discrepancy of the conductivity measurements between samples A and 2A seen in the figure above. The lesser-cured sample has a lower conductivity. Considering that samples E and 2E were uncured and also had lower conductivity than other samples, it can be hypothesized that the thermal conductivity of the material is affected by the amount of curing, with less curing resulting in a

lower thermal conductivity. This result can be justified by the molecular construction of the parts.

The Form II printer uses a UV laser to create solid layers of plastic out of liquid resin. When the parts undergo additional curing inside a box filled with UV light, the molecules within the parts have the chance to create further links and reinforce the connections between the molecules. Therefore, when heat is applied to both cured and uncured samples, the molecular and thermal responses will be different. Heat is transferred through the vibration of molecules and the cured parts with stronger and more numerous molecular bonds will transmit the heat more effectively as the vibrating molecules will transmit the vibrations faster.

While it is possible to justify the effect that curing has on the thermal properties of the additively manufactured parts, it does not account for the consistent variation in thermal conductivity across the various print locations on the build tray. Some possible explanations for the uneven distribution could include the effects of distance traveled by the UV waves on the accuracy and therefore intensity of the laser, an inconsistent temperature gradient across the build platform due to the placement of the printer in the lab, or the clarity of the various mirrors used to direct the laser to the resin covered build tray.

Chapter 5

Conclusions

This research yielded some important conclusions about the thermal conductivity of S.L.A. additively manufactured parts. For instance, we can conclude that the controllable variables involved in additive manufacturing do lead to variations in the thermal properties of plastic additively manufactured parts produced using SLA. The first step was to determine of accuracy of the TPS 500 used. By comparing the measured thermal conductivity with the value given by literature it was determined that the accuracy of the experiment procedure was 3.8%. Next the procedure was verified as being repeatable to within 2% by comparing the two sets of results taken for the same sample a month apart. At this point it was possible to analyze and justify the results collected.

By comparing the results for 25 μm and 100 μm, it was determined that the different layer thicknesses did yield different trends. The 25 μm results were more consistent across samples built in different orientations, while the 100 μm samples demonstrated a greater susceptibility to the build orientation variable. The next variable to be investigated was the part location on the build tray and through a second round of testing it was determined that the location on the build tray did influence the results and it was not tied to the shadows left on the build tray left by previous use. Instead, the degree to which the samples were cured was indicated to be an important variable. It was determined that a part that was less cured would have a lower thermal conductivity, while a part that had experienced more curing was better at transmitting heat. This deduction was justified by the crosslinking between molecules facilitated by the curing process and the fundamental concepts of heat transfer through particle vibration.

As a result of the unexpected results some of the variables in the samples were linked and the effects of each independent variable cannot be verified, therefore additional testing is required to verify the trends found in these results.

Recommendations for Future Research

While some this research was able to answer some questions, there are many more that still need to be examined. As seen above, theories were developed on the effects of layer thickness, print orientation, and cure time. It would be prudent to continue to examine these relationships to verify the results found here. The first step is to correct or adjust for the variation in the thermal conductivity across the build tray. Once the cause and effect of the print location issue are identified, the other results can be verified in a setting that keeps the variables truly independent.

Once that has been completed, the next step would be to determine whether the trends discovered hold true for other materials printed on the same printer or type of printer. This would determine if there are inherent differences because of the different material chemistries. The next expansion would be to examine other printing methods to determine whether the trends discovered are true for all additively manufactured parts. Based on the results obtained in this research, a reasonable hypothesis would be that both different materials and different manufacturing techniques will affect the trends seen. Parts constructed out of metals and other printing methods may not involve curing which will be fundamentally different from the experiment conducted here.

Appendix A

Selecting TPS Settings

Proper Settings

In order to input the correct and relevant test parameters follow the standard directions below.

Automatic Settings: These settings should remain constant between experiments

- Insulation: Kapton
- Cable: Grey
- Drift Enable: checkbox selected

Manual settings: These settings should be specified per experiment.

- Available probing depth: ½ of sample height
- Sensor design: 2.001mm, 3.002mm, or 6.004mm depending on sample size
- Sample Temperature: 20°C - steady state environmental temperature
- Measurement Time: 2.5-5 seconds (using longer times increases the necessary cooling wait time)
- Heating Power: 10mW-1W

Adjust measurement time and heating power until good data and reasonable calculated values appear with minimal error.

When you receive a “New Experiment” popup, as shown in Figure 17, describing the settings being employed by the sensor, check that the power and measurement times correct. Additionally, check the value for sensor resistance to ensure that it remains at a reasonable value (approximately between 1Ω and 15 Ω). Outrageously large or small numbers typically indicate an issue with the sensor or the gray cord to the sensor adaptor.

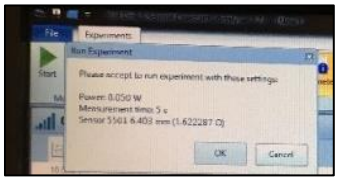

Figure 17: Confirmation pop-up window with experiment resistance

Example of Usable Results

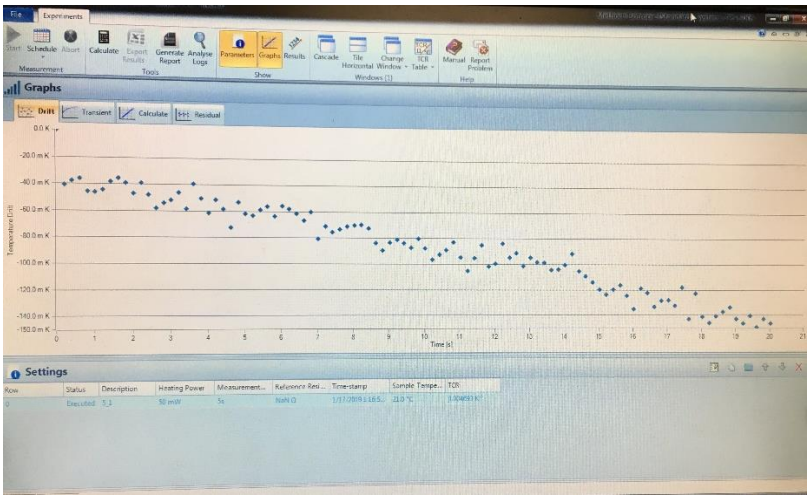

Figure 18: Example of "Drift" data with proper experimental setup

"Drift" data should have a soft trend with a fair degree of scatter as demonstrated in Figure 18.

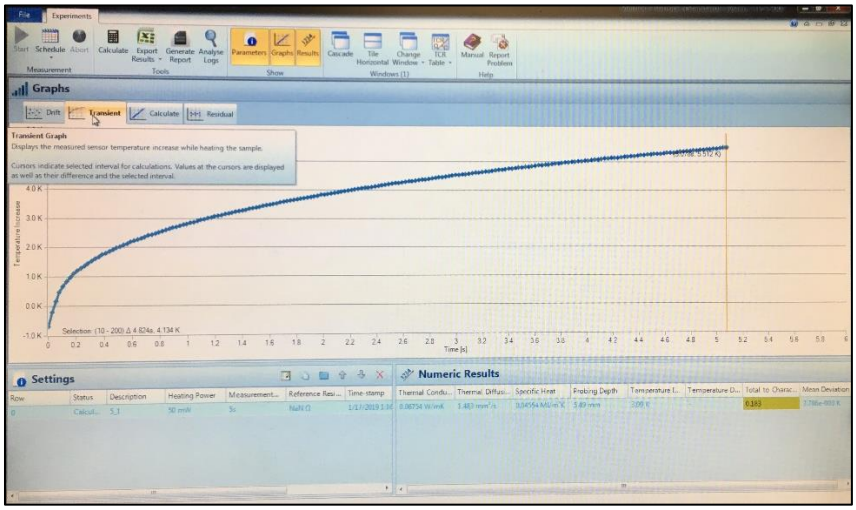

Figure 19: Example of "Transient" data with proper experimental setup

"Transient" data should appear as a curve as shown in Figure 19.

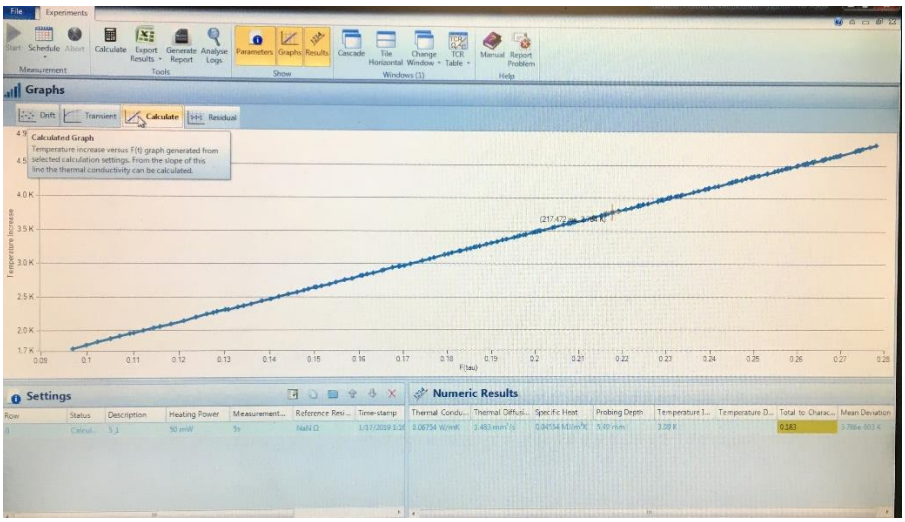

Figure 20: Example of "Calculate" data with proper experimental setup

"Calculate" data should consist of a straight line when the sample is loaded appropriately, and the sensor is functioning properly as shown in Figure 20.

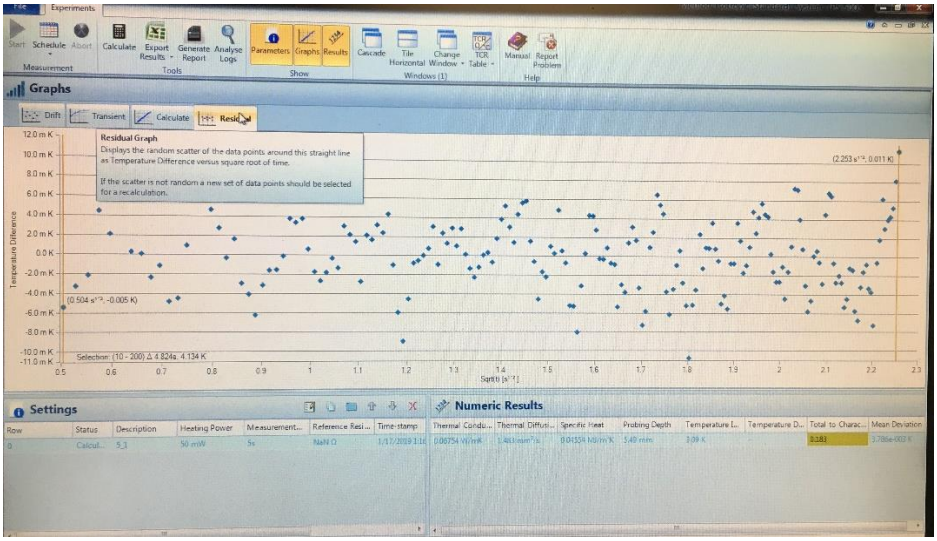

Figure 21: Example of "Residual" data with proper experimental setup

"Residual" data is a random scatter and has no visible trends as seen in Figure 21.

Example of Results Indicative of an Experimental Error

Sometimes the TPS sensor can be a bit finicky and will generate data that does not follow the proper trends, a few examples of which are included below.

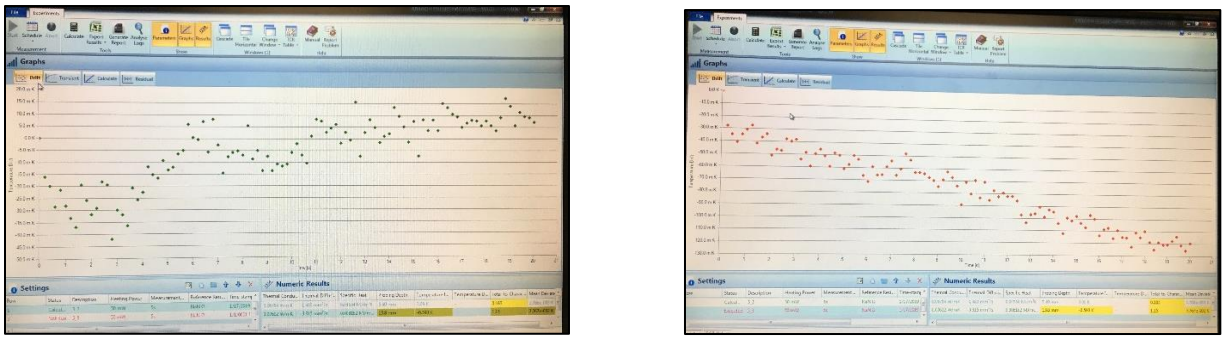

Figure 22: Results under "Drift" tab indicative of error

Figure 23: Results under "Calculate" tab indicative of error

Calculate should not show multiple lines unlike the trend demonstrated in Figure 23.

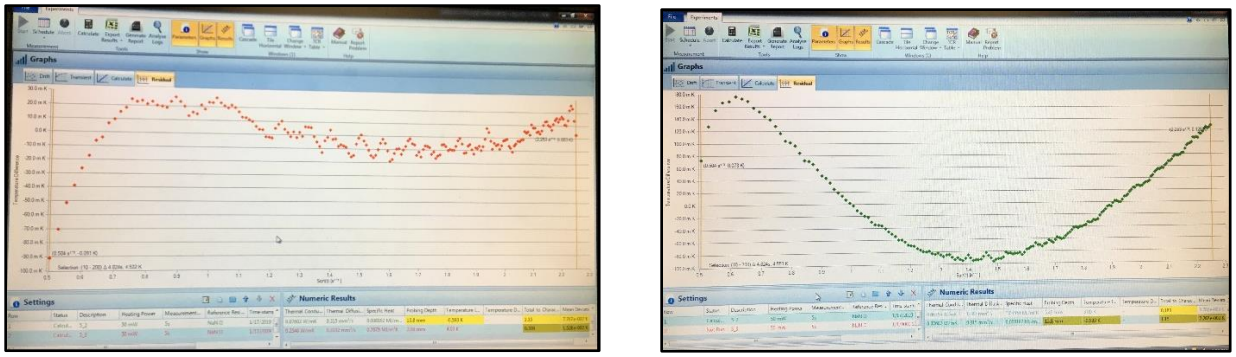

Figure 24: Results under "Residual" tab indicative of error.

Residual data should be random and should not follow any trend unlike the data in Figure 24.

If these trends appear, follow these troubleshooting tips:

- The sensor is properly mounted in its holder and the conductors are properly aligned as seen in the figure 8.
- Ensure your sample is centered and properly clamped as seen in figure 9.
- Untwist the gray cord so that the wires will come into proper contact with the sensor adaptor.
- Check the run variables you have input

Simplification of Running Process

In order to collect data in batches instead of taking each individual point individually, a schedule can be created. A schedule is a program that the computer will follow to the letter, so it is important to pay attention to the details.

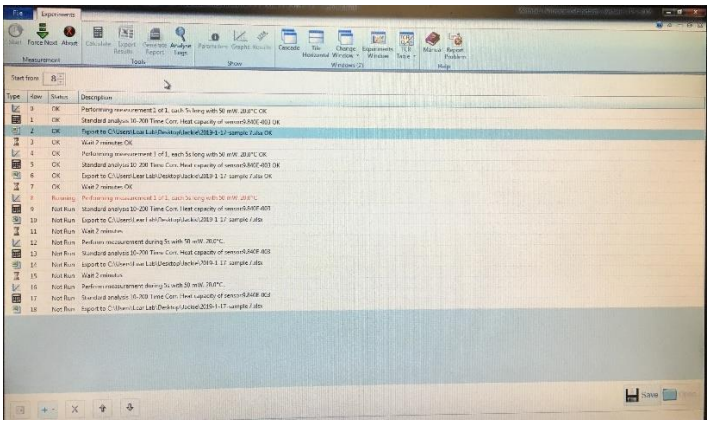

Figure 25: Run schedule with preset conditions and automatic export to Excel

To start a schedule, there must first be a saved run so that the computer knows where to store the data collected. Then once a new schedule is created, new events can be added. The first step should be to "Perform measurement," which by double clicking will allow you to set your proper run settings. The next step should be to simply run a "Standard analysis" on the data connection. In order to export directly to Excel, the command is "Export," which if you double click will ask you for a location and file type to save as. Finally, select the "Wait" option to schedule in pauses to allow the system to return to equilibrium. Once again, double click the event to customize the settings. Once these events have been created, they can be copied and pasted in the correct order for whatever number of runs will make-up the batch. Saving the schedule allows you to open and use that schedule again. When re-using a schedule, do not forget to adjust the schedule settings, especially the document address to which the results are exported.

BIBLIOGRAPHY

[1] J. Newman, “EADS, EOS Pair for AM Sustainability Study,” Digital Engineering, 05-Feb-2014. [Online]. Available: https://www.digitalengineering247.com/article/eads-eos-pair-for-am-sustainability-study/. [Accessed: 21-Mar-2017].

[2] B. Song, X. Zhao, S. Li, C. Han, Q. Wei, S. Wen, J. Liu, and Y. Shi, “Differences in microstructure and properties between selective laser melting and traditional manufacturing for fabrication of metal parts: A review,” *Frontiers of Mechanical Engineering*, vol. 10, no. 2, pp. 111–125, 2015.

[3] W. E. Frazier, “Metal Additive Manufacturing: A Review,” *Journal of Materials Engineering and Performance*, vol. 23, no. 6, pp. 1917–1928, 2014.

[4] J. F. Rodríguez, J. P. Thomas, and J. E. Renaud, “Mechanical behavior of acrylonitrile butadiene styrene (ABS) fused deposition materials. Experimental investigation,” *Rapid Prototyping Journal*, vol. 7, no. 3, pp. 148–158, 2001.

[5] M. Latouche, “SLA 3D Printing materials compared,” 3D Hubs. [Online]. Available: https://www.3dhubs.com/knowledge-base/sla-3d-printing-materials-compared. [Accessed: 26-Mar-2019].

[6] P. Michaleris, “Modeling metal deposition in heat transfer analyses of additive manufacturing processes,” *Finite Elements in Analysis and Design*, vol. 86, pp. 51–60, 2014.

[7] D. Buchbinder, H. Schleifenbaum, S. Heidrich, W. Meiners, and J. Bültmann, “High Power Selective Laser Melting (HP SLM) of Aluminum Parts,” *Physics Procedia*, vol. 12, pp. 271–278, 2011.

[8] “Photos & Videos,” Avonix Imaging. [Online]. Available: http://www.avoniximaging.com/photo-video-gallery. [Accessed: 25-Mar-2017].

[9]K. S. Prakash, T. Nancharaih, and V. S. Rao, “Additive Manufacturing Techniques in Manufacturing -An Overview,” *Materials Today: Proceedings*, vol. 5, no. 2, pp. 3873–3882, Mar. 2018.

[10] X. Wang, M. Jiang, Z. Zhou, J. Gou, and D. Hui, “3D printing of polymer matrix composites: A review and prospective,” *Composites Part B: Engineering*, vol. 110, pp. 442–458, Nov. 2016.

[11] B. Tymrak, M. Kreiger, and J. Pearce, “Mechanical properties of components fabricated with open-source 3-D printers under realistic environmental conditions,” *Materials & Design*, vol. 58, pp. 242–246, Feb. 2014.

[12] K. Chockalingam, N. Jawahar, and U. Chandrasekhar, “Influence of layer thickness on mechanical properties in stereolithography,” *Rapid Prototyping Journal*, vol. 12, no. 2, pp. 106–113, 2006.

[13] B. Wittbrodt and J. M. Pearce, “The effects of PLA color on material properties of 3-D printed components,” *Additive Manufacturing*, vol. 8, pp. 110–116, Oct. 2015.

[14] J. I. Jones, “The Synthesis Of Thermally Stable Polymers: A Progress Report,” *Journal of Macromolecular Science, Part C: Polymer Reviews*, vol. 2, no. 2, pp. 303–386, 1968.

[15] T. Flaata, G. J. Michna, and T. Letcher, “Thermal Conductivity Testing Apparatus for 3D Printed Materials,” *Volume 2: Heat Transfer Equipment; Heat Transfer in Multiphase Systems; Heat Transfer Under Extreme Conditions; Nanoscale Transport Phenomena; Theory and Fundamental Research in Heat Transfer; Thermophysical Properties; Transport Phenomena in Materials Processing and Manufacturing*, 2017.

[16] ASTM E1530-11(2016) Standard Test Method for Evaluating the Resistance to Thermal Transmission of Materials by the Guarded Heat Flow Meter Technique, *ASTM International,* 2016.

[17] Netzsch - Gerätebau GmbH, "Heat Flow Meter (HFM) and Guarded Hot Plate (GHP) Methods as Thermal Conductivity Measurements of Concrete ," Heat Flow Meter (HFM) and Guarded Hot Plate (GHP) Methods as Thermal Conductivity Measurements of Concrete.

[18] ASTM C177-13 Standard Test Method for Steady-State Heat Flux Measurements and Thermal Transmission Properties by Means of the Guarded-Hot-Plate Apparatus, *ASTM International,* 2013.

[19] G. Buonanno, A. Carotenuto, G. Giovinco, and N. Massarotti, "Experimental and Theoretical Modeling of the Effective Thermal Conductivity of Rough Steel Spheroid Packed Beds," *Journal of Heat Transfer*, vol. 125, no. 4, p. 693, 2003.

[20] ASTM C1043-16 Standard Practice for Guarded-Hot-Plate Design Using Circular Line-Heat Sources, *ASTM International*, 2016.

[21] "Hot Disk TPS 500," Thermtest Inc. [Online]. Available: https://www.thermtest.com/tps-500-theory-of-operation. [Accessed: 26-Apr-2017].

[22] ASTM D5930-16 Standard Test Method for Thermal Conductivity of Plastics by Means of a Transient Line-Source Technique, *ASTM International*, 2016.

[23] ASTM E1461-13 Standard Test Method for Thermal Diffusivity by the Flash Method, *ASTM International,* 2013.

[24] TA Instruments. (2014). Thermal Conductivity and Thermal Diffusivity [Brochure]. April 27, 2017.

[25] ASTM E1530-11(2016) Standard Test Method for Evaluating the Resistance to Thermal Transmission of Materials by the Guarded Heat Flow Meter Technique, *ASTM International*, 2016.

[26] M. G. Miller, J. M. Keith, J. A. King, R. A. Hauser, and A. M. Moran, "Comparison of the guarded-heat-flow and transient-plane-source methods for carbon-filled nylon 6,6 composites: Experiments and modeling," *Journal of Applied Polymer Science*, vol. 99, no. 5, pp. 2144–2151, 2005.

[27] TA Instruments. (2015). DTC-300 [Brochure]. Author. Retrieved November 13, 2017, from TA Instruments. DTC-300. DTC-300, 2015, www.tainstruments.com/wp-content/uploads/DTC-300_2015.pdf.

[28] TA Instruments. (2014). BROCH-Thermal Conductivity Diffusivity [Brochure]. Author. November 13, 2017, from http://www.tainstruments.com/wp-content/uploads/BROCH-ThermalConductivityDiffusivity-2014-EN-1.pdf

[29] Quotes for TPS 500 and DTC 300 [Telephone interview]. (2017, November 15).

[30] "TPS 500 (S)," Hot Disk. [Online]. Available: http://www.hotdiskinstruments.com/products-services/instruments/tps-500/. [Accessed: 12-Nov-2017].

[31]"Pyrex," *MIT Material Property Database*. [Online]. Available: http://www.mit.edu/~6.777/matprops/pyrex.htm. [Accessed: 25-Mar-2019].

[32]“Functional Prototyping Materials for Engineers,” *Formlabs*. [Online]. Available: https://formlabs.com/materials/engineering/#high-temp-resin. [Accessed: 26-Mar-2019].

[33] S. E. Gustafsson, “Transient plane source techniques for thermal conductivity and thermal diffusivity measurements of solid materials,” Review of Scientific Instruments, vol. 62, no. 3, pp. 797–804, 1991.

Academic Vita

Jacqueline Trautman

Jltrautman7@gmail.com

EDUCATION

Bachelor of Science in Mechanical Engineering
Schreyer Honors College
The Pennsylvania State University, University Park, PA
Graduation: **May 2019**
The University of Southampton, United Kingdom (Spring 2018)

TECHNICAL EXPERIENCE

Process Engineering Intern **June-Aug. 2018**
Pratt and Whitney, West Palm Beach, FL

- Partnered with assembly engineers and shop floor mechanics to build-up and teardown gas turbine jet engines in accordance with design specifications and development test requests
- Drafted a procedure to organize the method by which mechanics remove ancillary engine hardware during a teardown to increase efficiency and decrease the risk of damaging the engine

Test Engineering Intern **May-Aug. 2017**
Pratt and Whitney, East Hartford, CT

- Collaborated with engine operators, instrumentation, and process engineers to test and validate gas turbine jet engines and multiple component systems
- Developed borescoping manuals for each Pratt engine in service to standardize the inspection technique and guarantee consistent high-quality results

WORK EXPERIENCE

Smithsonian Engaging Girls in STEM Intern **May – Aug. 2016**
The National Air and Space Museum, Washington DC

- Evaluated Smithsonian STEM outreach programs regarding ability to attract / retain interest from K-12 girls and implemented modifications to existing outreach programs to optimize engagement
- Developed new educational STEM programing including new hands-on aeronautic engineering design challenges

SOFTWARE

AutoCAD Inventor SolidWorks MATLAB COMSOL

LEADERSHIP

VP Student Relations, Penn State Society of Women Engineers	2018-19
Lead, Penn State Women in Engineering Program (WEP)	2018-19
Member, Penn State Engineering Ambassadors	2017-19
Leader, "It's All About ME" Mentoring Program, American Society of Mechanical Eng.	2017-19
Mentor, Penn State WEP	2017-18
Leader, Penn State WEP Girl Scout Saturday Outreach	2015-18
Outreach Director, Penn State Society of Women Engineers	2016-18
Envoy, Penn State WEP	2016-17

HONORS

William & Wyllis Leonhard Honors Endowment Award	2015-19
Professor H.A. Everett Memorial Scholarship	2017
Best Engineering Design Award Lockheed Martin Design Project	2016
Penn State President's Freshmen Award	2016
American Nuclear Society Incoming Freshmen Award	2015